Graph cut liver segmentation for interstitial ultrasound therapy

Simon Esneault, Najah Hraiech, Eric Delabrousse, Jean-Louis Dillenseger

Graph Cut Liver Segmentation for Interstitial Ultrasound Therapy

Simon Esneault, Najah Hraiech, Éric Delabrousse, and Jean-Louis Dillenseger

***Abstract*— Within a specific medical application, the primary liver cancer curative treatment by a percutaneous high intensity ultrasound surgery, our study was designed to propose a fast 3D semi-automatic segmentation method of the liver, the tumor and the hepatic vascular networks. This method is characterized by a graph description of contrast medium injected CT volume where the links between the nodes describe either the degrees of similarity between voxels of the same class (region based approach) or the class changes between two neighboring voxels (boundary based approaches). The various weights describing these two properties are defined after a first interactive training phase. A Max-Flow/Min-Cut graph cut algorithm allowed partitioning the volume in two representative subsets of the segmented classes.**

I. Introduction

Hepatocellular carcinoma or primary liver cancer is a tumor that is relatively uncommon in the western states, although its incidence is rising [1]. It is the most common cancer in some parts of the world, with more than 1 million new cases diagnosed each year. At early stages, hepatocellular carcinoma is confined to a solitary mass in a portion of the liver and is so potentially curable by surgical resection [2]. Patients whose tumors are localized but unresectable due to its location in the liver, concomitant medical considerations (such as cirrhosis), or even limited bilateral tumors, may be candidates for percutaneous surgery (percutaneous ethanol injection, or radiofrequency) ablation for cancers smaller than 5 cm [3]. Besides these therapies, ultrasound surgery are now proposed within interstitial applicator context [4]. Besides other advantages, this therapy can be more precisely controlled in power and direction than the other one. But like any other minimally invasive image guided surgery, this procedure implies within the preoperative stage the definition of a precise planning and during the intervention itself the tracking and the control of the therapeutical effects.

The therapeutic ultrasound device is constituted by a small (3-4 mm width) planar ultrasonic mono-element transducer incorporated within a cylindrical interstitial applicator. The therapy itself is conducted as following: 1) the interstitial applicator is guided under ultrasound imaging within or on the boundary of the hepatic tumor ; 2) the therapy planning parameters (high intensity ultrasound shooting time and power, transducer rotation angle after each shot and the total transducer rotation) is applied in order to heat up and destroy the tumor. The final necrosis volume is directly related to the heat deposit. However this heating can be locally disturbed by the presence of blood vessels acting like coolers. It is thus important to define the anatomical framework as precisely as possible in order to locate the tumor within the liver and to specify its relations with the hepatic vascularization.

CT scans acquired at several time stages after contrast medium injection is the classical preoperative examination. Portal-venous phase imaging is usually sufficient to enhance the tumor and vascularization contrast. The objective of this paper is to present a fast semi-automatic segmentation method which enables to isolate the entire liver, the various hepatic vascular networks and the tumors.

II. Segmentation framework

We will consider the segmentation as the volume partitioning into 2 classes ”object” and ”background”. The presented method belongs to the class of semi-automatic segmentation tools for which some volume voxels are assigned in an interactive way to one of these two classes. This first labeling is then used as a training base for the volume final segmentation.

A number of problems in computer vision can be expressed as energy minimization. Within this class of methodologies, Greig et al. [5] then Boykov et al. [6] proposed an energy minimization method based on the partitioning of a graph into two subgraphs by a minimum cut/maximum flow algorithm (Min-Cut/Max-flow graph cut).

This graph partitioning algorithm can be perfectly adapted to our volume binary classification issue. Moreover, the transcription of our segmentation problematic into energy minimization makes it possible to encode various characteristics of our data: classification training, degree of similarity between voxels of the same class (region based approaches), changes between classes (boundary based approaches), and so on.

The segmentation problematic is described by a directional flow graph. The nodes set is defined by 2 particular nodes called terminal nodes and respectively representing the class ”object” and the class ”background”. The other nodes are intermediate nodes and correspond to the voxels of the 3D volume. Directed weighted links connect the nodes. The link topology and the initial weight assigned to these links are representative of the energy function to minimize.

In our case, the segmentation problematic is formulated by following energy function $E_T = \lambda \cdot E_{classif} + (1 - \lambda) \cdot E_{continuity}$ with $E_{classif}$,

S.Esneault and J.-L. Dillenseger are with INSERM, U642, Rennes, F-35000, France; and with Université de Rennes 1, LTSI, Rennes, F-35000, France {simon.esneault, jean-louis.dillenseger}@univ-rennes1.fr

N. Hraiech is with ANSYS, 69100 Villeurbanne, France; INSERM, U642, Rennes, F-35000, France; and with Université de Rennes 1, LTSI, Rennes, F-35000 France hraiech@gmail.com

E. Delabrousse is with INSERM, U556, Lyon, F-69003 France; and with Université Claude Bernard Lyon 1, Lyon, F-69000 France eric.delabrousse@tele2.fr

an energy coding the probability that a voxel belongs to the class "object" or "background" and $\mathrm{E}_{\mathrm{continuity}}$, an energy coding the degree of similarity or discontinuity between two neighboring voxels. The coefficient λ controls the balance between these two energy terms. The graph is build as following:

- The topological basis of $\mathrm{E}_{\mathrm{classif}}$ measurement. Each node representative of a voxel is connected by 2 links to the 2 terminal nodes. The weights associated to these links are representative of the membership probabilities to the class "object" and the class "background". These probabilities will be determined during the training phase.
- $\mathrm{E}_{\mathrm{continuity}}$ imposes the degree of similarity between neighbors encoding. Each node representative of a voxel is connected to its neighbors (in 6-connectivity or 26-connectivity) by links weighted by a function penalizing the dissimilarities.

The Max-Flow/Min-Cut algorithm [7] is applied on this graph in order to partition it into 2 subsets: the nodes associated to the terminal node "object" and those associated to the terminal node "background". The volume is so segmented.

III. Implementation

A. Training phase

The visual exploration of medical 3D volume by the 3 interactively selected sagittal, axial and coronal plans is classically used in clinical routine. On this visual basis using the mouse, the user interactively selects a set of voxels v_o that he considers belonging to the class "object", and others v_b, that he considers belonging to the class "background" (see Fig. 1). v_o and v_b have a double role: they will be used as seed points for the segmentation but also their value distribution (histograms) will serve as training basis for the $\mathrm{E}_{\mathrm{classif}}$ related initial weight assignment (see next section III-B).

B. $E_{classif}$ related initial weights

Let us take the case of the links coupling a node representative of a voxel v with value I to the terminal node "object". If v is a seed point, a predefined weight w_{cl_obj} will be assigned to the link. If v is unmarked, w_{cl_obj} will be representative to the "object" class membership probability $W_{object}(I)$.

$$w_{cl\_obj} = \begin{cases} \infty \text{ or a threshold value K} & \text{if } v \in v_o \\ 0 & \text{if } v \in v_b \\ \lambda \cdot W_{object}(I) & \text{elsewhere} \end{cases} \quad (1)$$

Similar, for the weight w_{cl_back} of the links coupling a node representative of voxel v to the terminal node "background".

$$w_{cl\_back} = \begin{cases} 0 & \text{if } v \in v_o \\ \infty \text{ or a threshold value K} & \text{if } v \in v_b \\ \lambda \cdot W_{bck}(I) & \text{elsewhere} \end{cases} \quad (2)$$

Contrary to the scheme described by Boykov et al. [7], [8], we will assign directly to $W_{object}(I)$ and $W_{bck}(I)$ the probability that v belongs to the 2 classes:

$$W_{object}(I) = \Pr(I/''\text{object}'') \quad (3)$$
$$W_{bck}(I) = \Pr(I/''\text{background}'') \quad (4)$$

The two probability distributions, $\Pr(I/''\text{object}'')$ and $\Pr(I/''\text{background}'')$ can be defined on an a priori basis or, as in our case, being deduced from the v_o et v_f value histograms. More precisely we propose several ways to extract the probability distributions from the histograms:

- The direct use of the histograms after normalization of their areas (or integrals). The histograms can be smoothed or not before normalization.
- The histogram modeling as a mixture of Gaussians. The user choose the number of Gaussians which fit the histograms by an Expectation-Maximization algorithm [9].

C. $E_{continuity}$ related initial weights

The weight of the links between two neighboring nodes, w_{cont}, must reflect the degree of similarity between voxels. The gray level gradient is commonly used as discontinuity marker. Boykov et al. suggest to use the following ad hoc function to establish the link weight between a voxel v_1 of value I_1 to v_2 of value I_2: $w_{cont} \propto \frac{\exp^{-(I_1-I_2)^2/2\sigma^2}}{\mathrm{dist}(v_1,v_2)}$ where $\mathrm{dist}(v_1,v_2)$ is the Euclidean distance between the two voxels and σ the measurement noise standard deviation [7]. We used the following proportionality ratios:

$$w_{cont} = (1-\lambda) \cdot A \cdot \frac{\exp^{-(I_1-I_2)^2/2\sigma^2}}{\mathrm{dist}(v_1,v_2)} \quad (5)$$

where A is a normalization constant which helps to keep an equal influence between the $E_{classif}$ and the $E_{continuity}$ related initial weights. $\mathrm{dist}(v_1,v_2)$ allows to process anisotropic data.

IV. Results

This algorithm has been tested on clinical abdominal CT volumes acquired at 4 different contrast medium diffusion phases. The volume properties are the following: each volume was composed by approximatively 120 512x512 pixel slices with a slice resolution of 0.77 mm and a slice thickness and an inter-slice spacing of 2 mm. This volume has been interpolated in order to recover an isotropic spacing.

The presented results have been performed on the parenchymatic phase volume but can be generalized on the other volumes. First a parallelepiped region of interest is interactively defined on two perpendicular slices in order to minimize the graph size. Fig. 1 shows the interactively selected learning seed points (in red -resp. green- the points belonging to the object -resp. background-).

$\Pr(I/''\text{object}'')$ has been defined as the sum of 2 Gaussians fitted on the histogram where $\Pr(I/''\text{background}'')$ has been defined by its smoothed normalized histogram

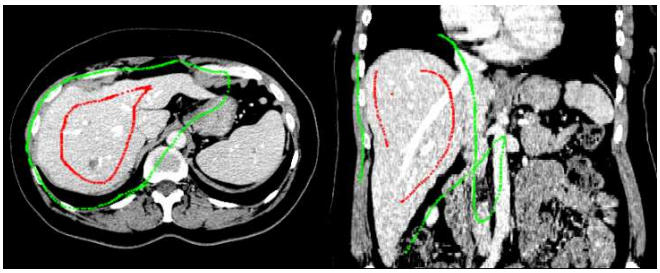

Fig. 1. Selected learning and seed points on the axial (left) and coronal (right) plans. In red the points belonging to the object and in green the points belonging to the background.

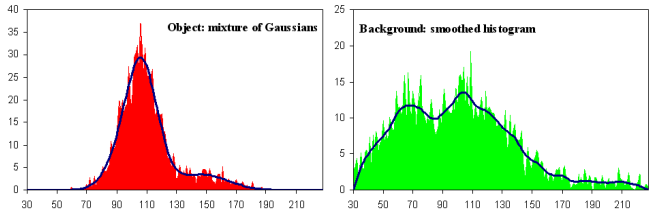

Fig. 2. $\Pr(I/''\text{object}'')$ (left) and $\Pr(I/''\text{background}'')$ (right) probability distributions.

(Fig. 2). The parameters $\lambda = 0.15$ and $\sigma = 5$ were selected in an ad hoc way.

After this training phase, the graph construction, the link weight assignments and the graph cut computation takes about 20 to 40 s on a 1.6 GHz Xeon Bi-Proc, 2 Go Ram PC. Sometimes some light post-processings have been applied (isolating biggest connected region, hole filling, etc.).

This process has been iteratively performed to extract the liver, the hepatic vascularization and the tumor.

Fig. 3 shows the extracted liver on a slice and on 3D visualization. The 3D volume rendering on Fig. 4 allows to see the tumor and the liver vascularization by transparency. The results presented on Fig. 5 are directly related on our medical application: the vascularization on the direct neighborhood of the tumor is shown from several viewing angles. This kind of results is one of the medical objective of our segmentation method and has a direct impact on the further therapy planning setting up.

Fig. 3. Visualization of the extracted liver: superimposed on a slice (left) and as a 3D visualization relatively to the ribs, spine and kidney (right).

Fig. 4. 3D volume rendering of the liver the tumor and the liver vascularization cans be seen by transparency.

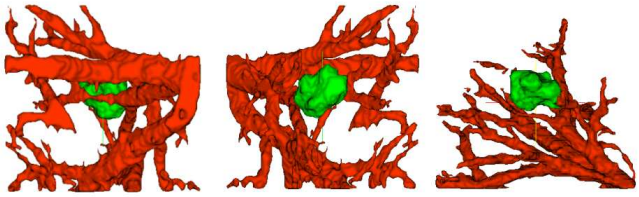

Fig. 5. Tumor and neighboring vascularization. View points from the front (left), back (center) and top (right).

V. Discussion

This class of approach has several critical points which have to be taken into account in order to perform a good segmentation.

- The number of training points and moreover the choice of their location has a direct influence on the results. Mainly two phenomena explain this influence:
  1) The quality of the estimated probability distributions. The selection of two many points can flatten the histograms, especially for heterogeneous regions. Also the 2 histograms should be constructed from almost the same number of points in order to build balanced probability distributions. The constant A of eq. 5 is also directly related to the number of selected points.
  2) The training points are seed points of the segmentation. In the case where two different structures are neighbor, a judicious seed points positioning can allow or not the segmentation.

  This imposes some little training of the user before achieving a specific task. However, the high interactivity level and the segmentation speed facilitate this phase.
- This method needs some parameters like λ or σ which are rather delicate to estimate and are dependant on the data set. Here also little training must be performed in order to choice these parameters in an ad hoc manner for a specific task.

A certain number of improvements are still under study to overcome some of these drawbacks.

However, this technique presents real benefits. It is sufficiently generic to be adapted easily to most of the segmentation tasks which can be found in several medical applications. The user interactivity level is rather weak compared to other manual driven segmentation. Moreover, this technique is fast enough to allow an immediate validation followed by an iterative interactive corrections.

VI. Conclusion

A fast 3D semi-automatic graph cut based segmentation method of the liver, the tumor and the hepatic vascular networks has been proposed. This method needs only little training of the interactions and is fast enough to be used within the clinical context. The obtained results will have a direct impact on establishing the therapy planning.

References

[1] H. B. El-Serag and A. C. Mason, "Rising incidence of hepatocellular carcinoma in the united states," *N Engl J Med*, vol. 340, no. 10, pp. 745–50, 1999.

[2] E. Mor, R. T. Kaspa, P. Sheiner, and M. Schwartz, "Treatment of hepatocellular carcinoma associated with cirrhosis in the era of liver transplantation," *Ann Intern Med*, vol. 129, no. 8, pp. 643–53, 1998.

[3] R. A. Lencioni, H. P. Allgaier, D. Cioni, M. Olschewski, P. Deibert, L. Crocetti, H. Frings, J. Laubenberger, I. Zuber, H. E. Blum, and C. Bartolozzi, "Small hepatocellular carcinoma in cirrhosis: randomized comparison of radio-frequency thermal ablation versus percutaneous ethanol injection," *Radiology*, vol. 228, no. 1, pp. 235–40, 2003.

[4] C. Lafon, J. Y. Chapelon, F. Prat, F. Gorry, Y. Theillere, and D. Cathignol, "Design and in vitro results of a high intensity ultrasound interstitial applicator," *Ultrasonics*, vol. 36, no. 1-5, pp. 683–7, 1998.

[5] D. M. Greig, B. T. Porteous, and A. H. Seheult, "Exact maximum a posteriori estimation for binary images," *J. Roy. Statist. Soc. B*, vol. 51, no. 2, pp. 271–279, 1989.

[6] Y. Boykov, O. Veksler, and R. Zabih, "Fast approximate energy minimization via graph cuts," *IEEE Trans Pattern Anal Mach Intell*, vol. 23, no. 11, pp. 1222–1239, 2001.

[7] Y. Boykov and M.-P. Jolly, "Interactive graph cuts for optimal boundary & region segmentation of objects in n-d images," in *8th Int. Conf. on Comp. Vis. ICCV'01*, vol. 1, (Vancouver), pp. 105–112, 2001.

[8] Y. Boykov and G. Funka-Lea, "Graph-cuts and efficient n-d image segmentation," *Int. J. Comp. Vis.*, vol. 70, no. 2, pp. 109–131, 2006.

[9] A. P. Dempster, N. M. Laird, and D. B. Rubin, "Maximum likelihood from incomplete data via the EM algorithm," *J. Roy. Statist. Soc. B*, vol. 39, no. 1, pp. 1–38, 1977.